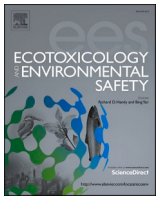
Ecotoxicology and Environmental Safety 305 (2025) 119180



Contents lists available at ScienceDirect

Ecotoxicology and Environmental Safety

journal homepage: www.elsevier.com/locate/ecoenv



Integrated model for heavy metal source tracing and multi-factor quantification, with risk assessment: A case study of a typical mega iron and steel enterprise in China

Xin Xu [a,b], Zheng Zhang [a,b], Peng Wang [a,b,c], Ziang Ma [a,b], Zhaotong Wang [a,b], Zimeng Zhao [a,b], Qing Wang [a,b], Xin Bo [a,b,*]

[a] Department of Environmental Science and Engineering, Beijing University of Chemical Technology, Beijing 100029, PR China
[b] BUCT Institute for Carbon-Neutrality of Chinese Industries, Beijing 100029, PR China
[c] Beijing Capital Air Environmental Science & Technology Co., Ltd., Beijing 100176, PR China

ARTICLE INFO

Edited by Richard Handy

Keywords:
Iron and steel industry
Heavy metals
Cross-media transport
Multi-factor quantification
Eco-health

ABSTRACT

The heavy industry sector is a major source of gaseous pollutants, including heavy metals (HMs), which disperse beyond enterprise boundaries and contaminate surrounding soils. However, soil heavy metal source tracing and multi-factor quantification of cross-media transport remain insufficient. To address these research gaps, an integrated model for heavy metal source tracing in soil beyond enterprise boundaries and multi-factor quantification was developed, with a case study of a typical mega iron and steel enterprise in Tangshan, Hebei Province, China. The results indicated that the CALPUFF model can effectively capture the cross-media transport of heavy metals and identify the spatial distribution patterns of heavy metal hotspots. Moreover, distance from pollution sources, soil physicochemical properties, and atmospheric deposition had different influences on HMs because of the variability in the properties of different HMs, with atmospheric deposition identified as the primary factor affecting As and Ni. The integrated ecological risk index (with an average RI value of 87.12) reflected a low cumulative ecological risk, with Cd, Tl, and Pb identified as the priority contributors over the other heavy metals. The probabilistic health risk assessment revealed that Cr was the primary contributor to carcinogenic risk, accounting for 69.80 % of the risk in adult males, 69.40 % of that in adult females, and 64.10 % of that in children, whereas Tl and Cr were the two major elements responsible for non-carcinogenic risk. This study provides a scientific basis for characterizing the source-sink dynamics of heavy metals and quantifying their cross-media transport under multiple influencing factors, thereby supporting the development of more effective pollution control and environmental management strategies in heavy industries, particularly the steel sector.

1. Introduction

The heavy industry sector significantly contributes to the emission of gaseous pollutants, including heavy metals, beyond enterprise boundaries, leading to soil contamination in surrounding areas. For example, the iron and steel industry (ISI) operates within an integrated production framework encompassing ore selection, sintering, coking, iron smelting, steelmaking, and steel rolling. The ISI requires substantial coal and coke consumption due to its inherently high resource and energy requirements (Cheng et al., 2020). During key manufacturing processes, smoke dust generated by both organized and unorganized emissions contains Fe, Zn, Ca, and Si in the form of simple or mixed oxides, alongside toxic heavy metals such as Mn, Ni, Cr, Cd, and Pb, which originate from raw materials or are introduced as additives (Dragović et al., 2014). These pollutants not only cause degradation and depletion of soil resources (Awual, 2017; Awual, 2019; Awual et al., 2020; Awual et al., 2019; Hasan et al., 2023b; Shahat et al., 2021) but also, through migration across environmental media or ingestion via the food chain, pose risks to ecosystems and public health (Awual, 2016; Awual et al., 2016; Hasan et al., 2023a; Salman et al., 2021; Salman et al., 2023). Consequently, investigating the cross-media release, dispersion, and deposition patterns of air pollutants from heavy industries, particularly the steel sector, is crucial for quantifying key influencing factors and assessing associated health risks. Such efforts provide essential insights

* Corresponding author at: Department of Environmental Science and Engineering, Beijing University of Chemical Technology, Beijing 100029, PR China.
E-mail address: boxin@buct.edu.cn (X. Bo).

https://doi.org/10.1016/j.ecoenv.2025.119180
Received 25 March 2025; Received in revised form 5 September 2025; Accepted 5 October 2025
0147-6513/© 2025 The Authors. Published by Elsevier Inc. This is an open access article under the CC BY-NC-ND license (http://creativecommons.org/licenses/by-nc-nd/4.0/).

for mitigating heavy metal pollution in steel production and developing strategic measures to address industrial environmental challenges effectively.

A key component of these efforts is understanding the cross-media transport pathways of pollutants, as this knowledge underpins the design of effective pollution control measures. Among these pathways, atmospheric emissions serve as a primary pathway for pollutant dispersion around industrial sites and are widely recognized as a major source of contamination because of their accumulation in surface soils (Luo et al., 2019). Heavy metals released from key steel industry processes into the atmosphere undergo transmission, diffusion, and chemical reactions before being ultimately deposited onto soil surfaces through dry and wet deposition, contributing significantly to soil pollution in areas surrounding steel enterprises (Ren et al., 2023; Sun et al., 2024; Yang et al., 2020). However, existing research has focused predominantly on site investigations and remediation efforts within steel plant boundaries (Dragović et al., 2014; Zhou et al., 2019). In contrast, studies addressing the cross-media impacts of heavy metal emissions from key steelmaking processes beyond plant boundaries are limited. Additionally, environmental impact assessments of air and soil media are often conducted separately, lacking a comprehensive, system-wide perspective on pollutant contributions from the steel industry. The mechanisms governing cross-media pollutant migration, encompassing atmospheric release (source), transport, diffusion, chemical transformations, and subsequent soil deposition (sink) through dry and wet deposition processes, have yet to be fully elucidated. Therefore, simulating the migration and deposition processes of atmospheric heavy metals, tracing their sources, and identifying key influencing factors in cross-media transfer play crucial roles in formulating effective pollution control strategies. These efforts are crucial for advancing cross-media pollution control technologies and promoting integrated environmental governance in heavy industries such as steel manufacturing.

Although the importance of investigating the cross-media behavior of heavy metals and identifying key influencing factors has been widely recognized, existing studies often remain limited in scope, focusing on individual factors or specific environmental media. For example, Chao et al. employed data science techniques to determine the relationships between natural factors and soil heavy metal concentrations and analyzed their influence on soil HM enrichment (Chao et al., 2025). Similarly, Qin et al. investigated the environmental impact of open-pit coal mining and the long-range transport of its pollutants, highlighting the need for preventive measures to protect fragile grassland ecosystems surrounding industrial regions (Qin et al., 2023). Shi et al. utilized the aforementioned models to simulate the dioxin effects from medical waste and incineration and validated the deposition effects through soil sampling analysis (Shi et al., 2020). Simulating the cross-media release, dispersion, and deposition processes of pollutants, along with tracing heavy metal sources and identifying key influencing factors, is essential for determining the distribution patterns of high-concentration pollutant deposition in soil. A more comprehensive, multidimensional approach is therefore needed to fully understand the interactions between atmospheric deposition and soil environments and to accurately identify the key factors influencing heavy metal accumulation in soils.

In identifying the source-sink characteristics of heavy metals across media, traditional regression models, while useful for revealing causal relationships, largely assume linear interactions between variables and thus struggle to capture the complex influence of multiple environmental factors on heavy metal distributions. Therefore, there is an urgent need to develop a predictive model capable of integrating multiple environmental variables, accommodating nonlinear relationships, and improving both predictive accuracy and generalizability. Notably, the feature importance derived from tree-based models effectively captures the nonlinear relationships between these factors, revealing their complex impact on heavy metal pollution (Auret and Aldrich, 2012; Wei et al., 2025). Unlike traditional linear models, tree-based models account for nonlinear interactions between variables through a recursive splitting mechanism, identifying key features strongly associated with heavy metal concentrations. Furthermore, the application of risk assessment methods based on soil heavy metal concentrations is crucial for conducting a systematic assessment of the soil pollution status. This study provides a scientific foundation for integrated soil contamination assessments and a theoretical foundation for developing effective soil pollution prevention and remediation strategies.

Based on this background, an integrated model was developed for heavy metal source tracing in soil beyond enterprise boundaries and multi-factor quantification, with a case study of a mega-iron and steel enterprise in Tangshan, Hebei Province, China. Unlike other studies, this study incorporated atmospheric deposition into the multi-factor quantification of heavy metal cross-media transport using tree-based models. This study aimed to simulate the migration, dispersion, and deposition processes of heavy metals across different media, identify high-deposition zones, quantify key factors influencing the migration of HMs, and conduct environmental assessments. The primary objectives were (1) to simulate the process of pollutant release, diffusion, and deposition of HMs using the CALPUFF model by integrating wind field data with pollution source information, accounting for both dry and wet deposition; (2) to validate the model's accuracy by comparing simulated data with actual monitoring data; (3) to perform heavy metal source tracing and quantify the effects of soil physicochemical properties, distance from emission sources, and simulated deposition flux on heavy metal concentrations; and (4) to evaluate the ecological risk by assessing the single pollution index (PI) and Nemerow pollution index (NPI) of HMs. Additionally, the carcinogenic and non-carcinogenic risks posed by HMs were quantified for both children and adults through three exposure pathways.

2. Materials and methods

This study developed an integrated model for source tracing of HMs in soil beyond enterprise boundaries and multi-factor quantification, with a case study of a mega iron and steel enterprise in Tangshan, Hebei Province, China. Specifically, the cross-media release, diffusion, and deposition of HMs in soil beyond the enterprise boundaries were simulated, and the influencing factors were quantified by considering the soil physicochemical properties, distance from emission sources, and simulated sedimentation flux. Feature importance was assessed using tree-based models. The framework of this study is illustrated in Fig. 1. The point and non-point input parameters of the CALPUFF model for the iron and steel enterprise were obtained from real-time data collected by continuous emission monitoring systems (CEMS), alongside information from environmental impact assessment (EIA) reports and emission permit implementation reports. Meteorological input parameters were obtained from a ground-based meteorological station located 7.1 km from the plant (Station ID: 54531). The CALPUFF model was subsequently used to forecast the dispersion range of HMs emitted during steel manufacturing, facilitating the calculation of the maximum ground-level pollutant concentrations. The maximum deposition area, determined by the combined effects of dry and wet deposition, was identified based on these predictions, and soil sampling points were established accordingly. The model's accuracy was validated by comparing the monitoring values with the model-simulated values. Furthermore, based on the deposition flux of HMs, an integrated model for source tracing of HMs and multi-factor quantification was developed. The influencing factors governing the cross-media release, diffusion, and deposition of pollutants were quantified, incorporating key soil physicochemical properties, distance from emission sources, and simulated sedimentation flux. Finally, the potential ecological risk was evaluated using the potential ecological risk index method to assess the ecological risk associated with individual heavy metals in the soil. Additionally, environmental exposure risks were quantified using a human health risk assessment model that considers three exposure pathways.

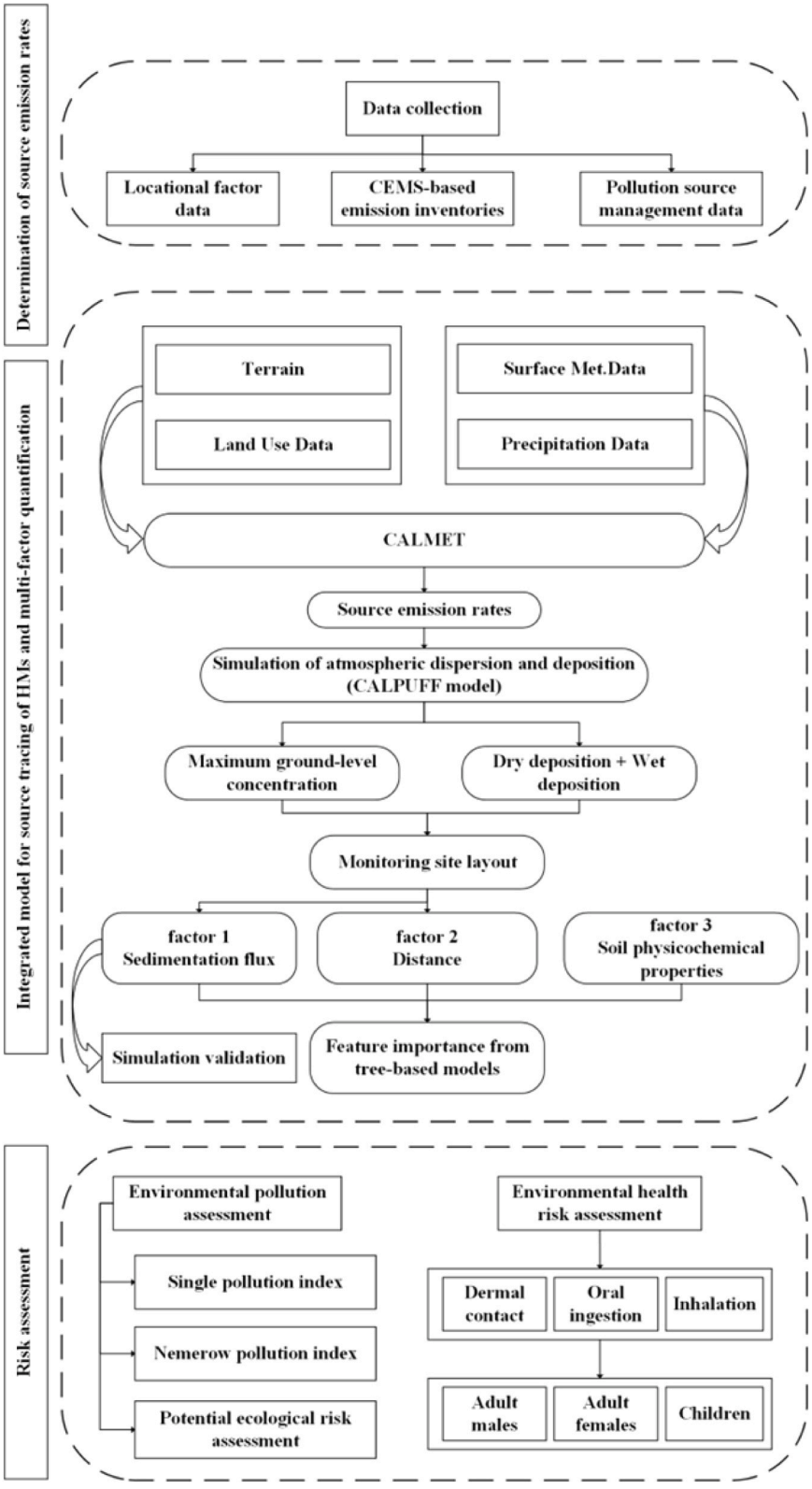


Fig. 1. Schematic diagram of the research framework.

2.1. Study area

Tangshan, a major coastal industrial city in eastern Hebei Province, stands as China's largest steel production center, housing more than 300 steel plants and a combined production capacity of 160 million tons (Yang et al., 2020). In this study, the selected study area encompassed a mega iron and steel enterprise in Tangshan and its surrounding region.

The enterprise is located in the Luanzhou Economic Development Zone of Hebei Province and operates as an integrated iron and steel enterprise, encompassing sintering, pelletizing, blast furnace iron-making, steelmaking, and rolling processes. The enterprise, covering an area of 120 hm^2 (Fig. 2), has an annual production capacity of 7 million

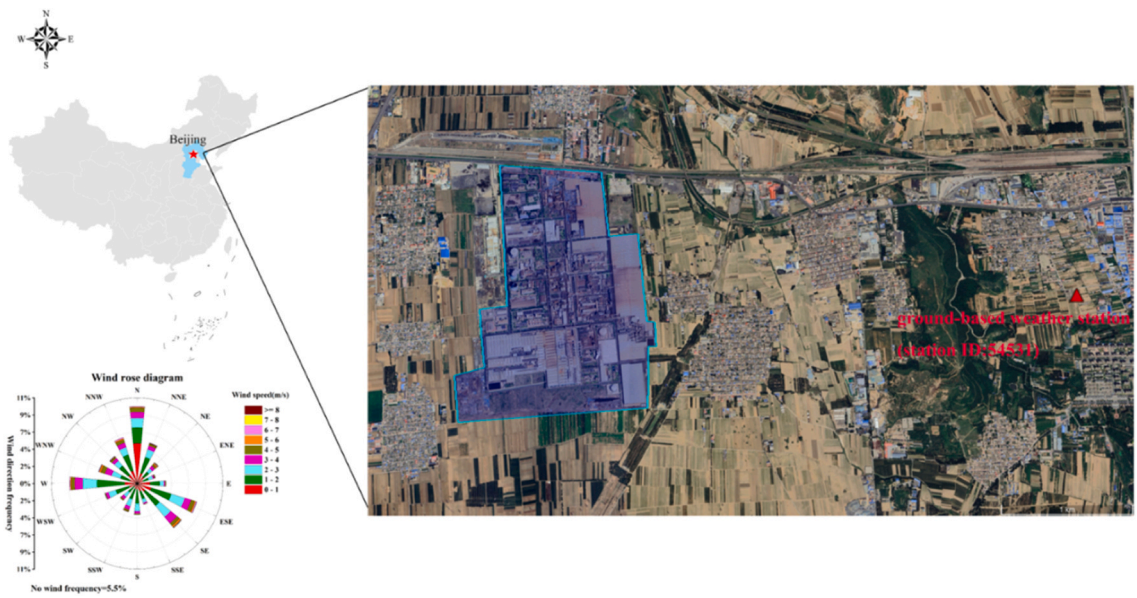


Fig. 2. Overview of the study area.

tons of sintered ore, 1.44 million tons of pelletized ore, 3.52 million tons of molten iron, and 3.6 million tons of molten steel.

The iron and steel enterprise is located in a hydrological-geological region of alluvial-fluvial plains characterized by flat terrain and gentle slopes. The predominant soil type is fluvo-aquic soil, which is weakly alkaline. The area experiences a warm-temperate, semi-humid monsoon continental climate with distinct seasons: dry and windy springs, hot and rainy summers, warm days and cool nights in autumn, and cold, snow-sparse winters. The main climatic parameters obtained from meteorological data collected over the past 20 years are summarized in Table S1.

2.2. Sampling and analysis

Given the challenges associated with directly measuring the cross-media deposition of heavy metals, this study adopted a numerical modeling approach, referencing the research conducted by Shi et al. (2020). In this study, the production output and emission control measures of the iron and steel enterprise remained generally stable during the period 2018–2024. Given that the 2018 emission data were of relatively higher quality and completeness (Bo et al., 2021), they were selected as the primary basis for this research.

It systematically accounts for both point and non-point source emissions from steel enterprises, treating emissions from factory chimneys as point sources. Point source emission data, including parameters such as chimney location, stack height, chimney diameter, flue gas exit velocity, flue gas exit temperature, and pollutant emission rates, were obtained from real-time measurements from continuous emission monitoring systems (CEMS). The calculation of non-point source emissions in 2018 has relied primarily on information provided in Environmental Impact Assessment (EIA) reports and Emission Permit Implementation Reports. Further, this study utilized the CALPUFF model to simulate the annual sedimentation flux of heavy metals during the normal production period of steel enterprises. Additionally, the calculation of the sedimentation amount takes into account the cumulative duration from the commencement of operations to the time of sampling and monitoring, incorporating the time scale factor. In the simulation process of CALPUFF, the emission rate parameters of non-point sources need to be considered. Owing to the lack of direct measurement data for non-point source emissions from different process units, this study estimated them using an area-based proportional allocation method. Specifically, the total non-point source emissions of each process were distributed to the corresponding areas according to the proportion of the workshop area occupied by that process. This method is based on the assumption that larger areas have greater potential for non-point source emissions. In the absence of measured data, this approach provides a reasonable approximation for the spatial allocation of emissions. The dispersion and sedimentation processes of heavy metals were subsequently simulated via CALPUFF model, with PM_{10} serving as a surrogate, and dry deposition and wet deposition were considered. The principle, composition, and application of the CALPUFF modeling system are presented in Text S1 of the Supporting Information. Furthermore, the selection of the soil monitoring sites (Fig. S1) was based on a comprehensive evaluation of the model results, meteorological conditions, and actual field observations.

The input parameters for the CALPUFF model consisted of terrain data, meteorological data, and emission source data (Table S2). The terrain data for the study area were obtained from the United States Geological Survey (USGS) Earth Resources Observation Systems (EROS) data center (www.usgs.gov/centers/eros)(Xu et al., 2023). The accuracy of the terrain data is 90 m, whereas the accuracy of the land use type data is 30 m (Bo et al., 2015; Wang et al., 2022). The upper-air meteorological data were derived from the three-dimensional meteorological field generated by the Weather Research and Forecasting (WRF) model (Guo et al., 2022). The ground-level meteorological data were provided by a ground-based meteorological station located 7.1 km from the plant (Station ID: 54531) and included parameters such as the wind direction, relative humidity, precipitation, temperature, wind speed, and air pressure. The simulation domain spanned 10 km × 10 km with a spatial resolution of 100 m. Due to the stable chemical properties of heavy metals, their decay or chemical transformation was not considered in the simulation. The specific model parameters are detailed in Tables S3–S4.

The soil samples were systematically collected in August 2024. The sampling points were arranged using a combination of professional judgment and systematic randomization methods. A total of 60 topsoil sampling points (0–20 cm) were designated based on the CALPUFF simulation results and actual site conditions. Sampling locations were selected in areas surrounding the steel enterprise where emission impacts were expected to be most significant, following the gradient of deposition flux predicted by the simulation (sampling points: 1–30). The arrangement of sampling points aimed to comprehensively cover potentially affected areas, ensuring that the collected data were both representative and extensive, facilitating an accurate assessment of iron

and steel enterprise emissions into the surrounding environment. In regions with higher deposition fluxes, additional sampling points were incorporated to increase the data density and accuracy, leading to a more precise evaluation. Additionally, 25 sampling points (sampling points 31–55) were evenly distributed within a 5 km radius of the steel plant to assess pollutant diffusion and deposition over a wider area and to analyze the spatial distribution of contamination. Furthermore, five control points (sampling points: 56–60) were established in areas distant from the steel plant, unaffected by emissions, to serve as background reference points for comparison with polluted areas. This approach enables the assessment of pollution levels and the identification of potential pollution sources. The geographical coordinates of all the sampling points were documented using GPS technology. The plum blossom point method was used to collect representative soil samples from each survey site. These samples were sealed in plastic bags for subsequent analysis of heavy metals (Cu, Cr, Ni, Zn, Pb, Cd, Tl, As, and Mn) in the soil. Details of the sampling analysis are presented in Text S2 of the Supporting Information.

2.3. The calculation of sedimentation values of HMs

The total sedimentation of heavy metals in the soil was calculated by considering the simulated annual sedimentation flux and the actual operational duration of the enterprise (Shi et al., 2020), which was calculated using Eq. (1).

$$\Delta C_j^{soil} = D_i \times T \tag{1}$$

where ΔC_j^{soil} represents the sedimentation value of HM j, g/m^2; D_i represents the sedimentation flux of PM_{10} at the i-th grid, g/m^2/s; and T represents the duration of the enterprise's operation.

2.4. Model evaluation methods

The model simulation results of heavy metal sedimentation in soil were validated by analyzing the correlation between model-simulated data and actual monitoring data, as recommended by the *Technical Guidelines for the Selection of Environmental Air Quality Models (Trial Version)*(Ministry of Ecology and Environment of the People's Republic of China, 2015). The correlation coefficient $R2$ between the soil monitoring values and model-simulated values was employed as the statistical indicator for model validation

(Shi et al., 2020). The correlation coefficient $R2$ was calculated using Eq. (2).

$$R^2 = \frac{\sum_{i=1}^{n}(O_i - \overline{O})(M_i - \overline{M})}{\sqrt{\sum_{i=1}^{n}(O_i - \overline{O})^2}\sqrt{\sum_{i=1}^{n}(M_i - \overline{M})^2}} \tag{2}$$

where O_i represents the actual soil monitoring values, mg/kg; $\overline{O}$ represents the average of the actual soil monitoring values across all sampling points, mg/kg; M_i represents the model-simulated sedimentation values, ng/m^2; $\overline{M}$ represents the average of the simulated sedimentation values across all sampling points, ng/m^2; and n is the number of sampling points.

2.5. Integrated model for heavy metal source tracing of HMs in soil beyond the boundaries of enterprises and multi-factor quantification

Heavy metals emitted from smokestacks of steel plants undergo atmospheric transmission, diffusion, and chemical reactions before ultimately accumulating in soil through dry and wet deposition, contributing significantly to soil pollution in areas surrounding steel plants. However, the soil environment functions as a buffer and filter for heavy metals entering its system. Previous studies have demonstrated that, based on soil characteristics and inherent mechanisms, soil ecosystems immobilize heavy metals through processes such as adsorption-desorption, redox reactions, and complexation reactions (Wang et al., 2024b; Yang et al., 2021). Among these mechanisms, the soil physicochemical factors affecting heavy metal behavior include pH, cation exchange capacity (CEC), and soil organic matter (SOM). Research has indicated that soil pH is negatively correlated with heavy metals, suggesting that lower pH levels result in increased heavy metal concentrations (Wang et al., 2024a). Conversely, SOM is positively correlated with heavy metal retention, suggesting that a reduction in organic matter content decreases the soil's capacity to adsorb heavy metals (Zhou et al., 2024). Additionally, the CEC significantly influences the ability of a soil to adsorb heavy metals, with a relatively high CEC enhancing the capacity of the soil to retain positively charged metal ions (Bradl, 2004; Lock and Janssen, 2003). The distance from the emission source to the sampling site also influences the extent of heavy metal deposition in the soil (Dragović et al., 2014).

This study developed an integrated model for source tracing of HMs in soil beyond enterprise boundaries and multi-factor quantification based on the deposition flux of HMs. Unlike other models, this integrated approach accounted for the effects of soil physicochemical properties, sedimentation flux, and the distance between the emission source and sampling points on the migration and deposition of pollutants. The importance scores of these influencing factors were quantified using feature importance derived from tree-based models. This methodology facilitates the analysis of factor contributions and interactions in heavy metal pollution, providing insights into the intricate influence of environmental factors on soil contamination and supporting the development of effective pollution control and environmental management strategies.

Spearman correlation analysis was conducted to examine the relationships between heavy metal concentrations in soil at different sampling points, soil physicochemical properties, distance from emission sources, and simulated sedimentation flux (Fig. S2). These findings provided scientific evidence for selecting key features in tree-based models for feature importance evaluation. Feature importance from tree-based models refers to the process of identifying significant features based on importance scores derived from models such as random forest (Roshanski et al., 2023). In these models, the contribution of each feature is determined by the reduction in the loss function when the feature is used for splitting a node. The algorithm traverses all nodes in the tree, calculates the reduction in the loss function for each feature at every split, and then aggregates these reductions to derive an overall importance score for each feature (Sirocchi et al., 2025). A higher feature importance score indicates a greater contribution of that feature to the model's predictive performance. This method is advantageous because it evaluates feature significance directly based on the data distribution and patterns without requiring complex transformations or assumptions. It is particularly suitable for large datasets with intricate relationships among features. The core formula for this process is as follows:

$$I_i = \sum_{t:v(t)=i} \Delta L_t \tag{3}$$

where Δt represents the reduction in loss at node t and where $v(t)$ denotes the feature i used for the split at node t.

In addition, three model evaluation metrics, namely, the root-mean-square error (RMSE), mean absolute error (MAE), and coefficient of determination (R^2), were selected to evaluate the performance and generalizability of the models. Detailed information about the model evaluation parameters can be found in Text S3.

2.6. Heavy metal pollution, ecological and health risk assessment

A single pollution index and the Nemerow pollution index were used

to evaluate heavy metal contamination in the study area. The potential ecological risk index method was used to assess the potential threats posed by individual heavy metals in the soil and the overall multi-factor risks within the study area. The assessment of health risks for adults and children considered both non-carcinogenic risk (NCR) and carcinogenic risk (CR) resulting from exposure to heavy metals. The standard model of the U.S. Environmental Protection Agency was used to evaluate these risks in relation to soil pollutant exposure, considering three primary exposure pathways: dermal contact, oral ingestion, and inhalation. Details of the calculation formulas and parameter selection are presented in Text S4 of the Supporting Information.

2.7. Quality assurance and control

The quality assurance and quality control (QA/QC) procedures were carried out using the CRM GBW07404a (GSS-4a), which was provided by the Center of National Standard Reference Material of China. The detection limits (mg/kg) for the measurements were as follows: Cu, Zn, and Mn at 1; Cr at 4; Ni at 3; Pb at 10 %; Cd and As at 0.01; and Tl at 0.1. To minimize background contamination, at least one blank control was included for every 10 samples. The relative standard deviation for replicate samples remained below 10 %, and the percentage recoveries for all HMs ranged from 93 % to 111 %, indicating that the procedures used to detect heavy metals in soil were relatively accurate and reliable.

2.8. Statistical analysis

All the raw data were analyzed using SPSS Statistics 25.0 (SPSS Inc., Chicago, IL, USA), and diagrams were generated via Origin 2025 software (Origin Lab Corp., Northampton, MA, USA). The map delineation was produced using ArcGIS 10.6, and the spatial distributions of the annual average sedimentation flux were visualized using Surfer 25. The analysis of influencing factors was based on tree-based models implemented with Python (version 3.7.4).

3. Results and discussion

3.1. Descriptive statistics and pollution levels of heavy metals

The soil pH varied between 7.49 and 9.83, with an average value of 8.48, which reflects the alkaline nature of the study area's soil. Furthermore, although the average concentrations of nine heavy metals were below the risk screening values specified in the "Soil Environmental Quality Risk Control Standard for Soil Contamination of Agricultural Land (GB15618–2018)" (SV) (MEEPRC, 2018), the concentrations at certain individual sampling sites exceeded the corresponding SVs (Table 1).

Table 1
Concentration of heavy metals (mg/kg) in soil samples collected from around the iron and steel enterprise.

	Max	Min	Mean	SD	N	n	DL	SV
Cu	27	3	9.03	4.13	60	4	1	100
Cr	324	14	76.87	76.13	60	4	4	250
Ni	28	5	12.65	5.87	60	4	3	190
Zn	681	15	68.63	86.66	60	4	1	300
Pb	315	11	23.42	38.60	60	4	10	170
Cd	3.86	0.04	0.16	0.49	60	4	0.01	0.6
Tl	6.9	0.2	0.54	0.84	60	4	0.1	/
As	8.16	2	4.08	1.27	60	4	0.01	25
Mn	5220	144	769.87	955.42	60	4	1	/

Notes: Max, maximum value; Min, minimum value; Mean, mean value; SD, standard deviation; N, number of samples detected; n, replicates; DL, detection limits; SV, soil environmental quality risk control standard for soil contamination of agricultural soil, China (GB15618–2018, Ministry of Ecology Environment of the People's Republic of China, 2018). The pH range of the soil samples from all the sampling points in this study was 7.49–9.83.

PI and NPI were utilized to evaluate the pollution levels of HMs and to further analyze their potential sources (Table S5). The average PI values for Cu, Ni, Zn, and As were 0.41, 0.41, 0.88, and 0.30, respectively, indicating a non-polluted level. In contrast, Cr, Pb, Cd, Tl, and Mn had average PI values of 1.13, 1.09, 1.66, 1.20, and 1.27, respectively, suggesting a slight pollution level (Fig. S3a). The NPI values for the nine HMs ranged from 0.14 to 1686.24. Among the collected samples, 3.33 % reached the moderately polluted level, 13.33 % were classified as highly polluted, and the remaining samples fell within the low pollution category, indicating the existence of localized contamination hotspots in the study area (Fig. S3b)

3.2. Simulation and validation of the CALPUFF model

The CALPUFF model was applied to simulate the release, dispersion, and deposition of heavy metals, thereby illustrating the cumulative deposition process (Fig. 3). The annual average sedimentation flux of HMs across the study area ranged from 0.03 to 29.73 ng/m^2/s, with the highest deposition levels observed in areas near the steel plant. This indicates more severe soil contamination in proximity to the source, whereas contamination levels declined significantly with increasing distance from the plant. This pattern highlights the localized nature of heavy metal deposition, which was primarily concentrated around industrial sources and is influenced by atmospheric dispersion conditions, wind speed, wind direction, and the mechanisms governing pollutant deposition. The deposition of heavy metals decreased markedly with increasing distance from the pollution source, a trend attributable to multiple factors, including particle size, turbulent atmospheric diffusion effects, and the physicochemical properties governing pollutant settling (Bai et al., 2016). Additionally, the simulation results demonstrated that variations in the local wind field played a significant role in shaping the dispersion and deposition patterns of pollutants. The prevailing wind direction throughout the year was from the north, with a secondary dominant wind from the west. As a result, the southern and eastern areas of the steel plant experienced relatively high levels of pollution, as pollutants were predominantly dispersed in these directions under the influence of wind patterns. These findings indicate that the distribution pattern of deposition flux was not solely determined by emission source strength but was also closely linked to regional meteorological conditions, which had a significant impact on the extent and direction of pollutant transport and deposition.

To evaluate the model's performance in simulating heavy metal deposition in soil, the correlation between model-simulated data and actual monitoring data was analyzed. The correlation coefficients (R^2) for various heavy metals are presented in Table S6 and range from 0.14 to 0.81. Among these, the R^2 values for Cu, Cr, Ni, and As exceeded 0.5. Notably,

As and Ni presented R^2 values of 0.81 and 0.71, respectively, demonstrating that the CALPUFF model effectively captured the cross-media transport of HMs. In contrast, the correlation coefficients for Zn, Pb, Cd, Tl, and Mn were notably lower, which may be attributed to the distinct migration characteristics of these HMs. Variations in their chemical properties, deposition velocities, and interactions with other substances in soil and air likely contributed to differences in atmospheric dispersion and deposition processes, potentially affecting the simulation results. Overall, the CALPUFF model effectively simulated pollutant transport and deposition by integrating meteorological conditions and emission source characteristics, achieving a high level of accuracy in capturing pollutant dispersion, deposition, and regional accumulation patterns. Previous studies have identified heavy metals commonly associated with steel plant emissions. Zhang et al. highlighted Cu, Cr, Ni, and As as typical pollutants emitted from steel plants (Zhang et al., 2022), whereas Zhou et al. identified Pb, Zn, and Cd as key heavy metals in the soil near such facilities (Zhou et al., 2019). Liu et al. further indicated that steel plants contribute to Tl pollution and that Mn is a significant heavy metal pollutant linked to these operations (Liu

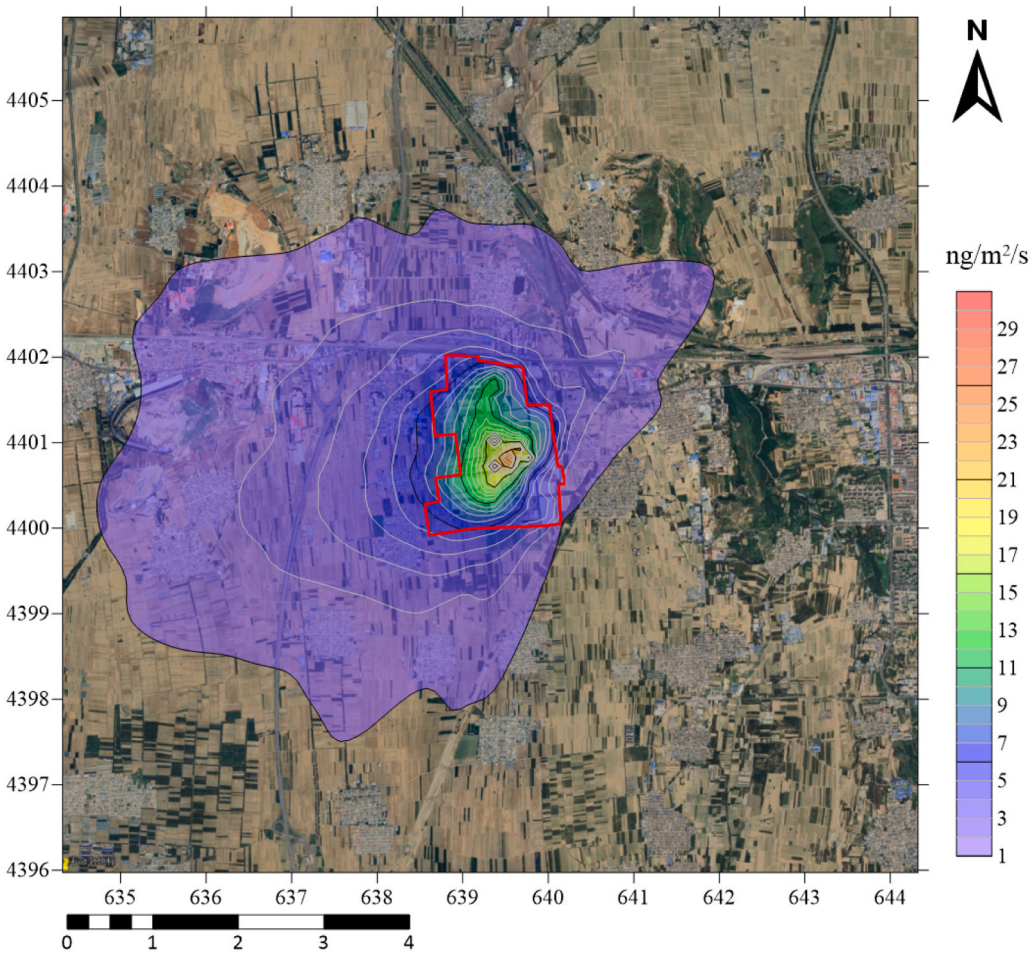


Fig. 3. Spatial distributions of the annual average sedimentation fluxes of HMs in the study area.

et al., 2017). Consistent with these findings, the simulation results in this study suggest that the Cu, Cr, Ni, Zn, Pb, Cd, Tl, As, and Mn in the soils surrounding the steel plant primarily originate from steel plant emissions. Spearman correlation analysis further supported these conclusions (Fig. S2).

3.3. Analysis of influencing factors using the integrated model

The key influencing factors were categorized into three groups: soil physicochemical properties (Awual et al., 2024; Hossain et al., 2024; Islam et al., 2025a; Islam et al., 2025b; Islam et al., 2025c; Islam et al., 2025d), distance from emission sources, and simulated sedimentation flux, which were the primary focus of the discussion. The feature importance of nine heavy metals with different properties was further analyzed using tree-based models. Importantly, the total sedimentation of different heavy metals in the soil was calculated based on the simulated annual sedimentation flux combined with the actual operation time of the enterprise. Therefore, both the sedimentation flux and the total sedimentation essentially reflected the sedimentation process of heavy metals in the soil. In light of this, sedimentation flux was selected as a key variable in the model input to more directly represent the sedimentation rates of heavy metals and their spatial distribution characteristics.

The tree-based models demonstrated satisfactory performance for each heavy metal, with R^2 values ranging from 0.63 to 0.96 (Table S7). The impact of influencing factors varied significantly depending on the specific heavy metal. Compared with pH, the cation exchange capacity (CEC) and soil organic matter (SOM) had more pronounced effects on heavy metals, particularly Cu, Zn, Pb, Cd, and Tl. CEC is closely related to the adsorption capacity of heavy metal ions, as it provides negatively charged exchange sites that effectively immobilize metal ions, reducing their mobility (Khaledian et al., 2017). For most heavy metals, including Cu, Pb, Cd, and Tl, the CEC was identified as the most influential factor, indicating its key role in regulating the mobility and stability of these metals in soils. Additionally, SOM, which contains organic ligands such as carboxyl and phenolic hydroxyl groups, can form stable organic complexes with Zn^{2+}, Cd^{2+}, and Tl^{+} (Li et al., 2023b). This process significantly enhances the capacity of SOM to retain these metals in soil, further enhancing their retention in soils. For As, the feature importance score of SOM was higher than that of CEC. In soil, As primarily exists in anionic forms (e.g., $HAsO_4^{2-}$, $H_2AsO_4^{-}$), and iron and aluminum oxides in soils adsorb As primarily through ligand exchange mechanisms (de Matos et al., 2001). Additionally, SOM can form stable complexes with As, reducing its mobility and bioavailability (Qiao et al., 2020). Furthermore, SOM influences soil pH, indirectly affecting the solubility and stability of As (Hussain et al., 2021). In soils with high organic matter content, SOM provides additional adsorption sites that compete with soil minerals for arsenic binding, thereby enhancing its immobilization.

pH was identified as the most influential factor for Mn, primarily because of its effect on Mn solubility and redox state (Li et al., 2021). In acidic soil environments, Mn predominantly exists in its soluble Mn^{2+} form, which is readily absorbed by plants. In contrast, in alkaline soils, Mn tends to form insoluble mineral compounds, such as MnO_2, thereby reducing its bioavailability. As a result, soil pH significantly influences the solubility, mobility, and bioavailability of Mn, playing a critical role in its environmental behavior. Similarly, pH was a key factor affecting chromium (Cr) in soils, as it determined its chemical speciation and

solubility (Jiang et al., 2025; Ullah et al., 2023). In acidic environments, Cr primarily exists as Cr^{3+}, a relatively stable form that readily binds to soil particles, forming insoluble complexes with low bioavailability. However, under alkaline conditions, Cr^{3+} can be oxidized to Cr^{6+}, a more soluble and toxic form that is easily absorbed by plants and microorganisms, increasing its environmental risk. Soil pH thus regulates the bioavailability, mobility, and potential ecological hazards of Cr by influencing its chemical transformation. These findings highlight the complexity of the interactions between metal chemical properties and soil factors, demonstrating the significant role of pH in governing the environmental behavior of Mn and Cr.

The distance from emission sources was a key factor affecting the distributions of Cu, Cr, Ni, Zn, Mn, and As, suggesting that these metals were significantly influenced by atmospheric pollution and deposition processes (Fig. 4). The correlation between the simulated deposition fluxes of these HMs and their measured soil concentrations ranged from 0.34 to 0.81, further confirming the crucial role of atmospheric deposition in their accumulation and spatial distribution in soil. Among these metals, As and Ni exhibited a stronger dependence on the deposition flux than distance, with feature importance scores exceeding 0.7 and 0.35, respectively. This finding indicated that diffusion and deposition processes were the dominant factors governing their environmental behavior (Li et al., 2023a; Liu et al., 2019). These findings align with previous studies identifying Ni and As as characteristic heavy metal pollutants associated with steel plants, further supporting the validity of the results.

Overall, the distribution of HMs was governed by multiple factors, with the interaction between distance from emission sources, soil physicochemical properties, and atmospheric deposition playing a particularly significant role.

3.4. Assessment of potential ecological risk and health risk

3.4.1. Potential ecological risk assessment

The ecological risk assessment results indicated that Cu, Cr, Ni, Zn, Pb, Tl, As, and Mn presented minimal ecological risk, with 100.0 % of the samples showing E_r^i values less than 40, indicating low risk (Table S8 and Fig. S4a). In contrast, Cd posed a greater ecological risk, with 83.33 % of the samples categorized as low risk, 15.00 % as moderate risk, and 1.67 % as considerable risk. The average E_r^i value for Cd was 49.68, indicating that it was the primary pollutant contributing to the ecological risk (Fig. S4b). The integrated ecological risk index (with an average RI value of 87.12) reflected a low cumulative ecological risk. Among all the samples, 98.33 % were classified as low risk, whereas 1.67 % fell within the moderate risk category. From the perspective of individual ecological risk indices, Cd, Tl, and Pb posed greater ecological risks compared to other heavy metals and were the major contributors and significantly contributed to the overall ecological risk index.

3.4.2. Health risk assessment

The probability distributions of carcinogenic risk (TCR) and non-carcinogenic risk (NCR) for adult males, adult females, and children are presented in Fig. 5. For carcinogenic risk, both the 95th percentile and the average TCR values for adult males and adult females exceeded 1E-04, indicating that the soil heavy metals in the study area posed a carcinogenic risk to adult health (Fig. 5a). Similarly, the 95th percentile TCR values for children also exceeded 1E-04, suggesting a carcinogenic risk for children in the study area. Additionally, TCR values exceeding the unacceptable threshold of 1E-04 were observed in about 56.67 % of the adult males, 63.33 % of the adult females, and 13.33 % of the

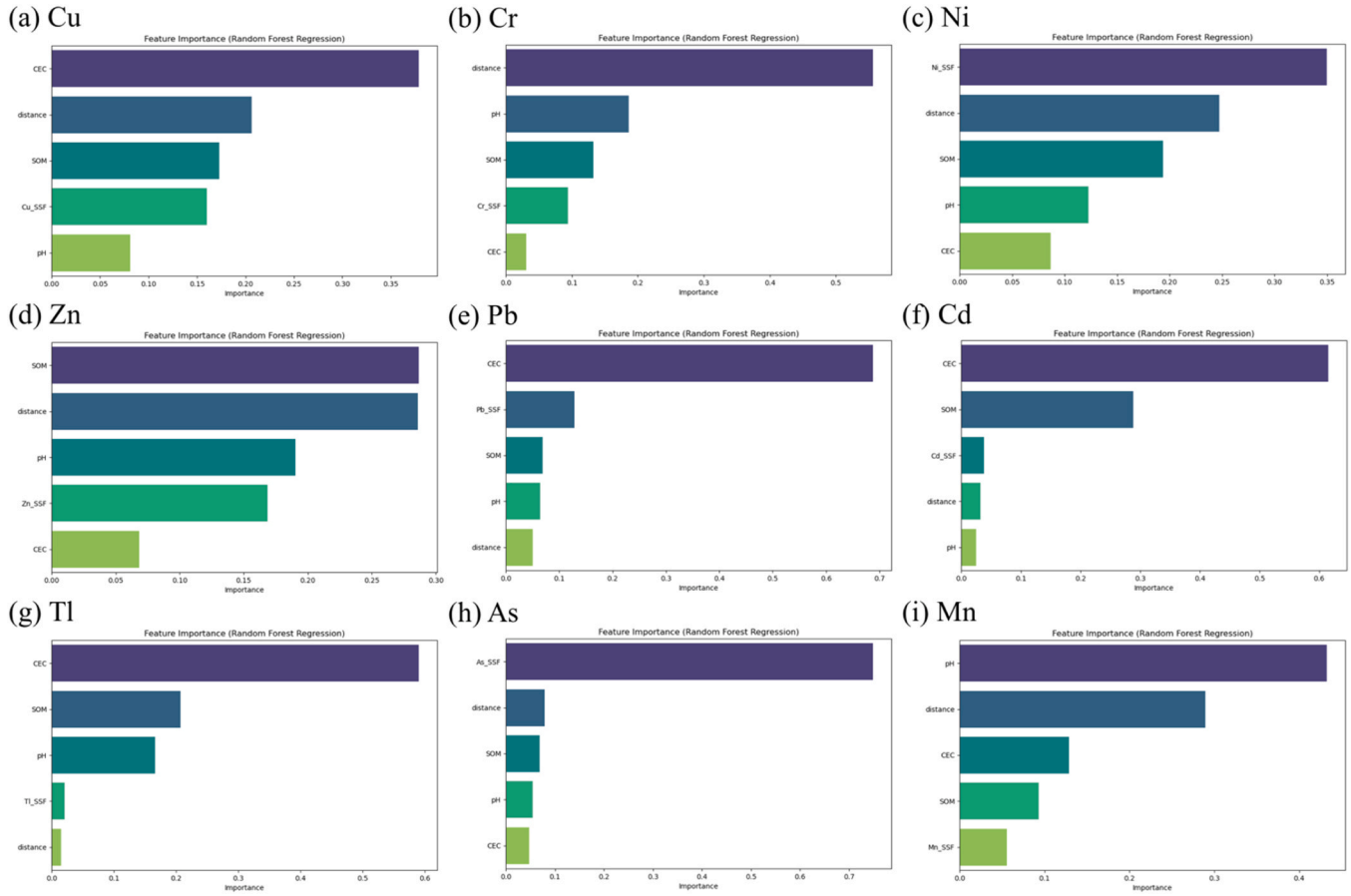


Fig. 4. Feature importance scores based on tree-based models for (a) Cu, (b) Cr, (c) Ni, (d) Zn, (e) Pb, (f) Cd, (g) Tl, (h) As, and (i) Mn. Notes: SSF represents the simulated sedimentation flux.

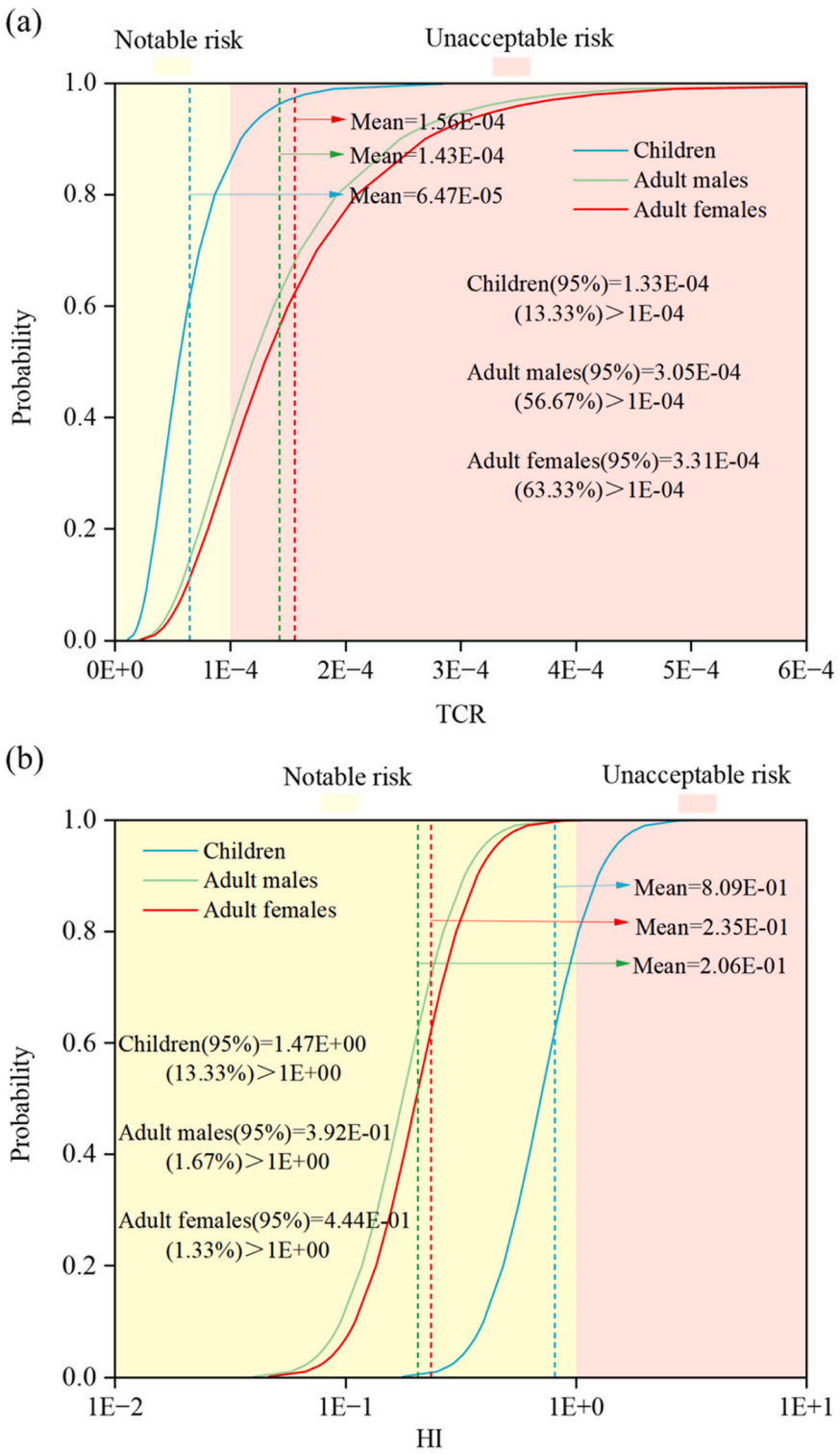


Fig. 5. (a) Probability distribution of the TCR for children and adults (a) and probability distribution of the hazard index (HI) for children and adults (b).

children, indicating that carcinogenic risk was a concern in the study area. Cr was the primary contributor to carcinogenic risk, accounting for 69.80 % of the risk in adult males, 69.40 % in adult females, and 64.10 % in children (Fig. S5a-c). The combined contribution of Ni, Pb, Cd, and As to the TCR in adults and children exceeded 30 %.

The average HI value for adults (adult males and adult females) remained below 1, with the 95th percentile HI values recorded at 3.92E-01 for adult males and 4.44E-01 for adult females (Fig. 5b). Additionally, 1.67 % of the HI values for adults exceeded the threshold of 1. While the average HI value for children was also below 1, the 95th percentile HI value reached 1.47E+ 00, with 13.33 % of HI values surpassing the threshold of 1, indicating that the NCR to children was not negligible (Yuan et al., 2023). Among the contributing elements, Tl accounted for 37.10 %, 38.10 %, and 43.50 % of the non-carcinogenic risk in adult males, adult females, and children, respectively, whereas Cr contributed 27.40 %, 27.20 %, and 23.20 %, respectively, making them the two primary elements responsible for NCR (Fig. S6a-c). The aggregate contribution of other heavy metals in soil (Cu, Ni, Zn, Pb, Cd,

As, and Mn) to non-carcinogenic risk in both adults and children surpassed 30 %.

4. Conclusions

This study developed an integrated model for heavy metal source tracing in soil beyond enterprise boundaries and multi-factor quantification of cross-media transport, with a case study of a mega iron and steel enterprise in Tangshan, Hebei Province, China. Additionally, an ecological risk and probabilistic human health risk assessment was conducted. The results showed that the CALPUFF simulation demonstrated strong performance in capturing the cross-media transport of heavy metals and identifying the spatial distribution patterns of heavy metal hotspots. Unlike previous studies, this study incorporated atmospheric deposition into the multi-factor quantification of heavy metal cross-media transport using tree-based models, and atmospheric deposition for As and Ni had a greater impact compared with other heavy metals. Moreover, the effects of soil physicochemical properties varied across different metals, reflecting the distinct characteristics of each heavy metal. The distance from emission sources was identified as a non-negligible factor influencing the cross-media transport behavior of Cu, Cr, Ni, Zn, Mn, and As. of their cross-media transport behavior. Furthermore, the integrated ecological risk index (with an average RI value of 87.12) reflected a low cumulative ecological risk, with Cd, Tl, and Pb identified as the dominant contributors among the assessed heavy metals. The probabilistic health risk assessment revealed that the carcinogenic risk for adults and children was at an unacceptable level and that Cr was the primary contributor to the carcinogenic risk for different population groups. Tl and Cr were identified as the dominant contributors to non-carcinogenic risk, highlighting their critical role in driving potential health concerns.

This study highlights the necessity of assessing heavy metal exposure in soils beyond the boundaries of iron and steel enterprises. This study successfully identified high-deposition zones resulting from the cross-media migration of heavy metals emitted during key manufacturing processes and quantified the critical factors influencing heavy metal migration across media using an integrated model. The findings provide a scientifically robust framework for heavy metal source tracing and quantifying influencing factors, offering significant insights for environmental risk management in heavy industries, particularly the steel sector. Future research could incorporate additional potential influencing factors to conduct more detailed and comprehensive analyses and to further advance the understanding of heavy metal cross-media transport.

CRediT authorship contribution statement

Xin Xu: Writing – original draft, Visualization, Validation, Software, Project administration, Methodology, Investigation, Formal analysis, Data curation. **Zheng Zhang:** Software, Methodology, Investigation, Conceptualization. **Peng Wang:** Software, Methodology, Data curation. **Ziang Ma:** Software, Data curation, Conceptualization. **Zhaotong Wang:** Visualization, Supervision, Investigation. **Zimeng Zhao:** Investigation, Conceptualization. **Qing Wang:** Data curation, Conceptualization. **Xin Bo:** Writing – review & editing, Supervision, Resources, Funding acquisition, Conceptualization.

Ethical approval

This article does not contain any studies with human participants or animals performed by any of the authors.

Declaration of Competing Interest

The authors declare that they have no known competing financial interests or personal relationships that could have appeared to influence the work reported in this paper.

Acknowledgments

This work was supported by grants from the National Natural Science Foundation of China (No. 72174125) and the Fundamental Research Funds for the Central Universities (buctrc202133).

Appendix A. Supporting information

Supplementary data associated with this article can be found in the online version at doi:10.1016/j.ecoenv.2025.119180.

Data availability

Data will be made available on request.

References

Auret, L., Aldrich, C., 2012. Interpretation of nonlinear relationships between process variables by use of random forests. Min. Eng. 35, 27–42. https://doi.org/10.1016/j.mineng.2012.05.008.

Awual, M.R., 2016. Solid phase sensitive palladium (II) ions detection and recovery using ligand based efficient conjugate nanomaterials. Chem. Eng. J. 300, 264–272. https://doi.org/10.1016/j.cej.2016.04.071.

Awual, M.R., 2017. New type mesoporous conjugate material for selective optical copper (II) ions monitoring & removal from polluted waters. Chem. Eng. J. 307, 85–94. https://doi.org/10.1016/j.cej.2016.07.110.

Awual, M.R., 2019. Mesoporous composite material for efficient lead (II) detection and removal from aqueous media. J. Environ. Chem. Eng. 7 (3), 103124. https://doi.org/10.1016/j.jece.2019.103124.

Awual, M.R., Hasan, M.M., Iqbal, J., Islam, M.A., Islam, A., Khandaker, S., Asiri, A.M., Rahman, M.M., 2020. Ligand based sustainable composite material for sensitive nickel (II) capturing in aqueous media. J. Environ. Chem. Eng. 8 (1), 103591. https://doi.org/10.1016/j.jece.2019.103591.

Awual, M.R., Hasan, M.M., Khaleque, M.A., Sheikh, M.C., 2016. Treatment of copper (II) containing wastewater by a newly developed ligand based facial conjugate materials. Chem. Eng. J. 288, 368–376. https://doi.org/10.1016/j.cej.2015.11.108.

Awual, M.R., Islam, A., Hasan, M.M., Rahman, M.M., Asiri, A.M., Khaleque, M.A., Chanmiya Sheikh, M., 2019. Introducing an alternate conjugated material for enhanced lead (II) capturing from wastewater. J. Clean. Prod. 224, 920–929. https://doi.org/10.1016/j.jclepro.2019.03.241.

Awual, M.E., Salman, M.S., Hasan, M.M., Hasan, M.N., Kubra, K.T., Sheikh, M.C., Rasee, A.I., Rehan, A.I., Waliullah, R.M., Hossain, M.S., Marwani, H.M., Asiri, A.M., Rahman, M.M., Islam, A., Khaleque, M.A., Awual, M.R., 2024. Ligand imprinted composite adsorbent for effective Ni(II) ion monitoring and removal from contaminated water. J. Ind. Eng. Chem. 131, 585–592. https://doi.org/10.1016/j.jiec.2023.10.062.

Bai, J., Jia, J., Zhang, G., Zhao, Q., Lu, Q., Cui, B., Liu, X., 2016. Spatial and temporal dynamics of heavy metal pollution and source identification in sediment cores from the short-term flooding riparian wetlands in a Chinese delta. Environ. Pollut. 219, 379–388. https://doi.org/10.1016/j.envpol.2016.05.016.

Bo, X., Jia, M., Xue, X., Tang, L., Mi, Z., Wang, S., Cui, W., Chang, X., Ruan, J., Dong, G., Zhou, B., Davis, S.J., 2021. Effect of strengthened standards on Chinese ironmaking and steelmaking emissions. Nat. Sustain 4, 811–820.

Bo, X., W, G., Tian, J., Yang, J., Gao, X., Huang, Y., Li, S., 2015. Standard systems of surface parameters in AERMOD. China Environ. Sci. 35 (9), 2570–2575.

Bradl, H.B., 2004. Adsorption of heavy metal ions on soils and soils constituents. J. Colloid Interface Sci. 277, 1–18. https://doi.org/10.1016/j.jcis.2004.04.005.

Chao, J., Gu, H., Liao, Q., Zuo, W., Qi, C., Liu, J., Tian, C., Lin, Z., 2025. Natural factor-based spatial prediction and source apportionment of typical heavy metals in Chinese surface soil: application of machine learning models. Environ. Pollut. 366, 125373. https://doi.org/10.1016/j.envpol.2024.125373.

Cheng, Z., Tan, Z., Guo, Z., Yang, J., Wang, Q., 2020. Recent progress in sustainable and energy-efficient technologies for sinter production in the iron and steel industry. Renew. Sus. Energ. Rev. 131, 110034. https://doi.org/10.1016/j.rser.2020.110034.

Dragović, R., Gajić, B., Dragović, S., Đorđević, M., Đorđević, M., Mihailović, N., Onjia, A., 2014. Assessment of the impact of geographical factors on the spatial distribution of heavy metals in soils around the steel production facility in smederevo (Serbia). J. Clean. Prod. 84, 550–562. https://doi.org/10.1016/j.jclepro.2014.03.060.

Guo, X., Li, S., Zhang, Y., Wu, B., Guo, W., 2022. Applications of dynamic simulation for source analysis of soil pollutants based on atmospheric diffusion and deposition model. Sci. Total Environ. 839, 156057. https://doi.org/10.1016/j.scitotenv.2022.156057.

Hasan, M.M., Kubra, K.T., Hasan, M.N., Awual, M.E., Salman, M.S., Sheikh, M.C., Rehan, A.I., Rasee, A.I., Waliullah, R.M., Islam, M.S., Khandaker, S., Islam, A., Hossain, M.S., Alsukaibi, A.K.D., Alshammari, H.M., Awual, M.R., 2023a. Sustainable ligand-modified based composite material for the selective and effective cadmium (II) capturing from wastewater. J. Mol. Liq. 371, 121125. https://doi.org/10.1016/j.molliq.2022.121125.

Hasan, M.M., Salman, M.S., Hasan, M.N., Rehan, A.I., Awual, M.E., Rasee, A.I., Waliullah, R.M., Hossain, M.S., Kubra, K.T., Sheikh, M.C., Khaleque, M.A., Marwani, H.M., Islam, A., Awual, M.R., 2023b. Facial conjugate adsorbent for sustainable pb (II) ion monitoring and removal from contaminated water. Colloid Surf. A 673, 131794. https://doi.org/10.1016/j.colsurfa.2023.131794.

Hossain, M.S., Shenashen, M.A., Awual, M.E., Rehan, A.I., Rasee, A.I., Waliullah, R.M., Kubra, K.T., Salman, M.S., Sheikh, M.C., Hasan, M.N., Hasan, M.M., Islam, A., Khaleque, M.A., Marwani, H.M., Alzahrani, K.A., Asiri, A.M., Rahman, M.M., Awual, M.R., 2024. Benign separation, adsorption, and recovery of rare-earth yb (III) ions with specific ligand-based composite adsorbent. Process Saf. Environ. 185, 367–374. https://doi.org/10.1016/j.psep.2024.03.026.

Hussain, M.M., Bibi, I., Niazi, N.K., Shahid, M., Iqbal, J., Shakoor, M.B., Ahmad, A., Shah, N.S., Bhattacharya, P., Mao, K., Bundschuh, J., Ok, Y.S., Zhang, H., 2021. Arsenic biogeochemical cycling in paddy soil-rice system: interaction with various factors, amendments and mineral nutrients. Sci. Total Environ. 773, 145040. https://doi.org/10.1016/j.scitotenv.2021.145040.

Islam, A., Islam, M.T., Teo, S.H., Mahmud, H., Swaraz, A.M., Rehan, A.I., Rasee, A.I., Kubra, K.T., Hasan, M.M., Salman, M.S., Waliullah, R.M., Hasan, M.N., Sheikh, M.C., Uchida, T., Awual, M.E., Hossain, M.S., Znad, H., Awual, M.R., 2025a. Progress in silicon-based materials for emerging solar-powered Green hydrogen (H_2) production. Adv. Colloid Interface 343, 103558. https://doi.org/10.1016/j.cis.2025.103558.

Islam, A., Malek, A., Islam, M.T., Nipa, F.Y., Raihan, O., Mahmud, H., Uddin, M.E., Ibrahim, M.L., Abdulkareem-Alsultan, G., Mondal, A.H., Hasan, M.M., Salman, M.S., Kubra, K.T., Hasan, M.N., Sheikh, M.C., Uchida, T., Rasee, A.I., Rehan, A.I., Awual, M.E., Hossain, M.S., Waliullah, R.M., Awual, M.R., 2025b. Next frontier in photocatalytic hydrogen production through CdS heterojunctions. Int J. Hydrog. Energ. 101, 173–211. https://doi.org/10.1016/j.ijhydene.2024.12.300.

Islam, A., Shahriar, M., Islam, M.T., Teo, S.H., Khan, M.A.R., Taufiq-Yap, Y.H., Mohanta, S.C., Rehan, A.I., Rasee, A.I., Kubra, K.T., Hasan, M.M., Salman, M.S., Waliullah, R.M., Hasan, M.N., Sheikh, M.C., Uchida, T., Awual, M.E., Hossain, M.S., Znad, H., Awual, M.R., 2025c. Advances in filler-crosslinked membranes for hydrogen fuel cells in sustainable energy generation. Int. J. Hydrog. Energ. 140, 745–776. https://doi.org/10.1016/j.ijhydene.2025.05.197.

Islam, A., Teo, S.H., Islam, M.T., Mondal, A.H., Mahmud, H., Ahmed, S., Ibrahim, M., Taufiq-Yap, Y.H., G, A.-A., Hossain, M.L., Sheikh, M.C., Rasee, A.I., Rehan, A.I., Waliullah, R.M., Awual, M.E., Hasan, M.M., Hossain, M.S., Kubra, K.T., Salman, M. S., Hasan, M.N., Awual, M.R., 2025d. Harnessing visible light for sustainable biodiesel production with Ni/Si/MgO photocatalyst. Renew. Sust. Energ. Rev. 208, 115033. https://doi.org/10.1016/j.rser.2024.115033.

Jiang, Y., Hu, C., Zhou, A., Qiu, H., Cao, B., Xu, J., 2025. Effectiveness of various chemical leaching systems in the remediation of chromium-contaminated soil and their impact on chromium speciation. J. Environ. Sci. China. https://doi.org/10.1016/j.jes.2025.02.012.

Khaledian, Y., Brevik, E.C., Pereira, P., Cerdà, A., Fattah, M.A., Tazikeh, H., 2017. Modeling soil cation exchange capacity in multiple countries. CATENA 158, 194–200. https://doi.org/10.1016/j.catena.2017.07.002.

Li, H., Santos, F., Butler, K., Herndon, E., 2021. A critical review on the multiple roles of manganese in stabilizing and destabilizing soil organic matter. Environ. Sci. Technol. 55 (18), 12136–12152. https://doi.org/10.1021/acs.est.1c00299.

Li, S., Wang, B., Zhang, X., Wang, H., Yi, Y., Huang, X., Gao, X., Zhu, P., Han, W., 2023b. Soil particle aggregation and aggregate stability associated with ion specificity and organic matter content. Geoderma 429, 116285. https://doi.org/10.1016/j.geoderma.2022.116285.

Li, D., Zheng, J., Yang, M., Meng, Y., Yu, X., Zhou, H., Tong, L., Wang, K., Li, Y.-F., Wang, X., Xiao, H., 2023a. Atmospheric wet deposition of trace metal elements: monitoring and modelling. Sci. Total Environ. 893, 164880. https://doi.org/10.1016/j.scitotenv.2023.164880.

Liu, J., Luo, X., Wang, J., Xiao, T., Chen, D., Sheng, G., Yin, M., Lippold, H., Wang, C., Chen, Y., 2017. Thallium contamination in arable soils and vegetables around a steel plant—A newly-found significant source of tl pollution in south China. Environ. Pollut. 224, 445–453. https://doi.org/10.1016/j.envpol.2017.02.025.

Liu, H.-L., Zhou, J., Li, M., Hu, Y.-m, Liu, X., Zhou, J., 2019. Study of the bioavailability of heavy metals from atmospheric deposition on the soil-pakchoi (Brassica chinensis L.) system. J. Hazard Mater. 362, 9–16. https://doi.org/10.1016/j.jhazmat.2018.09.032.

Lock, K., Janssen, C.R., 2003. Influence of aging on copper bioavailability in soils. Environm. Toxicol. Chem. Int. J. 22, 1162–1166. https://doi.org/10.1002/etc.5620220527.

Luo, X., Bing, H., Luo, Z., Wang, Y., Jin, L., 2019. Impacts of atmospheric particulate matter pollution on environmental biogeochemistry of trace metals in soil-plant system: a review. Environ. Pollut. 255, 113138.

de Matos, A.T., Fontes, M.P.F., da Costa, L.M., Martinez, M.A., 2001. Mobility of heavy metals as related to soil chemical and mineralogical characteristics of Brazilian soils. Environ. Pollut. 111 (3), 429–435. https://doi.org/10.1016/S0269-7491(00)00088–9.

MEEPRC (Ministry of Ecology Environment of the People's Republic of China), 2018. Chinese Soil Environmental Quality-Risk Control Standard for Soil Contamination of Agricultural Land (GB 15618–2018) (in Chinese).

Ministry of Ecology and Environment of the People's Republic of China, Technical Guidelines for the Selection of Environmental Air Quality Models (Trial Version), 2015. ⟨https://www.mee.gov.cn/gkml/hbb/bgth/201508/W020150911488652824265.pdf⟩(accessed 29 August 2025).

Qiao, W., Guo, H., He, C., Shi, Q., Xiu, W., Zhao, B., 2020. Molecular evidence of arsenic mobility linked to biodegradable organic matter. Environ. Sci. Technol. 54 (12), 7280–7290. https://doi.org/10.1021/acs.est.0c00737.

Qin, M., Jin, Y., Peng, T., Zhao, B., Hou, D., 2023. Heavy metal pollution in Mongolian-Manchurian grassland soil and effect of long-range dust transport by wind. Environ. Int. 177, 108019. https://doi.org/10.1016/j.envint.2023.108019.

Ren, H., Dong, W., Zhang, Q., Cheng, J., 2023. Identification of priority pollutants at an integrated iron and steel facility based on environmental and health impacts in the Yangtze river delta region, China. Ecotox Environ. Safe 264, 115464. https://doi.org/10.1016/j.ecoenv.2023.115464.

Roshanski, I., Kalech, M., Rokach, L., 2023. Automatic feature engineering for learning compact decision trees. Expert Syst. Appl. 229, 120470. https://doi.org/10.1016/j.eswa.2023.120470.

Salman, M.S., Hasan, M.N., Kubra, K.T., Hasan, M.M., 2021. Optical detection and recovery of yb (III) from waste sample using novel sensor ensemble nanomaterials. Microchem. J. 162, 105868. https://doi.org/10.1016/j.microc.2020.105868.

Salman, M.S., Sheikh, M.C., Hasan, M.M., Hasan, M.N., Kubra, K.T., Rehan, A.I., Awual, M.E., Rasee, A.I., Waliullah, R.M., Hossain, M.S., Khaleque, M.A., Alsukaibi, A.K.D., Alshammari, H.M., Awual, M.R., 2023. Chitosan-coated cotton fiber composite for efficient toxic dye encapsulation from aqueous media. Appl. Surf. Sci. 622, 157008. https://doi.org/10.1016/j.apsusc.2023.157008.

Shahat, A., Kubra, K.T., Salman, M.S., Hasan, M.N., Hasan, M.M., 2021. Novel solid-state sensor material for efficient cadmium (II) detection and capturing from wastewater. Microchem J. 164, 105967. https://doi.org/10.1016/j.microc.2021.105967.

Shi, M., Bo, X., Tian, F., Yang, Z., Wang, G., Ma, G., Jia, Y., Li, S., Zhu, B., 2020. Study on deposition effects of dioxins based on different air quality models. China Environ. Sci. 40, 24.

Sirocchi, C., Urschler, M., Pfeifer, B., 2025. Feature graphs for interpretable unsupervised tree ensembles: centrality, interaction, and application in disease subtyping. BioData Min. 18 (1), 15. https://doi.org/10.1186/s13040-025–00430-3.

Sun, H., Jia, X., Wu, Z., Yu, P., Zhang, L., Wang, S., Xia, T., 2024. Contamination and source-specific health risk assessment of polycyclic aromatic hydrocarbons in soil from a mega iron and steel site in China. Environ. Pollut. 340, 122851. https://doi.org/10.1016/j.envpol.2023.122851.

Ullah, S., Liu, Q., Wang, S., Jan, A.U., Sharif, H.M.A., Ditta, A., Wang, G., Cheng, H., 2023. Sources, impacts, factors affecting cr uptake in plants, and mechanisms behind phytoremediation of Cr-contaminated soils. Sci. Total Environ. 899, 165726. https://doi.org/10.1016/j.scitotenv.2023.165726.

Wang, C., Chu, Y., Ruan, J., Sang, M., Cheng, J., Wu, C., Bo, X., 2022. Research on the influence of AERMOD model surface parameter update on simulation effect. China Environ. Sci. 42, 2070.

Wang, Y., Zhang, Z., Li, Y., Liang, C., Huang, H., Wang, S., 2024a. Available heavy metals concentrations in agricultural soils: relationship with soil properties and total heavy metals concentrations in different industries. J. Hazard Mater. 471, 134410. https://doi.org/10.1016/j.jhazmat.2024.134410.

Wang, Z., Zhou, T., Wu, Y., Tan, Z., 2024b. A review of the electrochemical coupled leaching technique: an effective solution for remediation of heavy metal contaminated soils. Rev. Environ. Contam. T 262, 17. https://doi.org/10.1007/s44169-024–00068-y.

Wei, Q., Chen, Y., Zhang, H., Jia, Z., Yang, J., Niu, B., 2025. Simulation and prediction of PM2.5 concentrations and analysis of driving factors using interpretable tree-based models in shanghai, China. Environ. Res. 270, 121003. https://doi.org/10.1016/j.envres.2025.121003.

Xu, X., Wang, C., Wang, P., Chu, Y., Guo, J., Bo, X., Lin, A., 2023. Bioaerosol dispersion and environmental risk simulation: method and a case study for a biopharmaceutical plant of gansu province, China. Sci. Total Environ. 860, 160506. https://doi.org/10.1016/j.scitotenv.2022.160506.

Yang, H., Huang, K., Zhang, K., Weng, Q., Zhang, H., Wang, F., 2021. Predicting heavy metal adsorption on soil with machine learning and mapping global distribution of soil adsorption capacities. Environ. Sci. Technol. 55, 14316–14328. https://doi.org/10.1021/acs.est.1c02479.

Yang, L., Li, S., Wen, T., Meng, F., Chen, G., Qian, X., 2020. Influence of ferrous-metal production on Mercury contamination and fractionation in farmland soil around five typical iron and steel enterprises of tangshan, China. Ecotox Environ. Safe 188, 109774. https://doi.org/10.1016/j.ecoenv.2019.109774.

Yuan, B., Cao, H., Du, P., Ren, J., Chen, J., Zhang, H., Zhang, Y., Luo, H., 2023. Source-oriented probabilistic health risk assessment of soil potentially toxic elements in a typical mining city. J. Hazard Mater. 443, 130222. https://doi.org/10.1016/j.jhazmat.2022.130222.

Zhang, X., Yang, H., Sun, R., Cui, M., Sun, N., Zhang, S., 2022. Evaluation and analysis of heavy metals in iron and steel industrial area. Environ. Dev. Sustain. 24, 10997–11010. https://doi.org/10.1007/s10668-021–01893-0.

Zhou, T., Bo, X., Qu, J., Wang, L., Zhou, J., Li, S., 2019. Characteristics of PCDD/Fs and metals in surface soil around an iron and steel plant in north China plain. Chemosphere 216, 413–418. https://doi.org/10.1016/j.chemosphere.2018.10.024.

Zhou, W., Li, Z., Liu, Y., Shen, C., Tang, H., Huang, Y., 2024. Soil type data provide new methods and insights for heavy metal pollution assessment and driving factors analysis. J. Hazard Mater. 480, 135868. https://doi.org/10.1016/j.jhazmat.2024.135868.